https://doi.org/10.1016/j.geomorph.2016.05.019

Elsevier Editorial System(tm) for Geomorphology
Manuscript Draft

Manuscript Number: GEOMOR-5687R3

Title: Tectonic and morphosedimentary features of the 2010 Chile earthquake and tsunami in Arauco Gulf and Mataquito River (Central Chile)

Article Type: Research Paper

Keywords: 2010 Chile tsunami; coseismic deformation; uplift; tsunami deposits

Corresponding Author: Dr. Javier Lario, Ph.D.

Corresponding Author's Institution: Universidad Nacional de Educación a Distancia

First Author: Javier Lario, Ph.D.

Order of Authors: Javier Lario, Ph.D.; Cari Zazo, Professor; José L Goy, Professor

Abstract: Effects of the 2010 Chilean earthquake and tsunami were evaluated at coastal sites between two zones of different coseismic deformation. Land deformation, run up, inundation extent and deposit extent and thickness were measured in the field, providing insights into the processes and morphological changes associated with tsunami inundation and backwash. Three to five waves, of height up to 10 m, deposited several related layers along the coast, the thickness of these sandy deposits never exceed 80 cm, and is generally less than 30 cm. Coseismic deformation measured by means of bio- and geomorphic markers agrees well both with model deformation and measured GPS. There is no relationship between the run up height and the trend of coseismic deformation (uplift or subsidence), mainly because the effects of the tsunami were influenced locally by offshore bathymetry and coastal morphology.

Highlights

- Land deformation, run up, inundation extent and deposit extent and thickness were measured in the field after the 2010 Chilean earthquake and tsunami.
- Coseismic deformation measured by means of bio- and geomorphic markers agrees well both with model deformation and measured GPS.
- No relationship was found between coseismic land deformations, tsunami run-up and sedimentological features.

Tectonic and morphosedimentary features of the 2010 Chile earthquake and tsunami in the Arauco Gulf and Mataquito River (Central Chile).

J. Lario[1,*], C. Zazo[2], J.L. Goy[3]

1. Facultad de Ciencias, Universidad Nacional de Educación a Distancia (UNED), 28040-Madrid, Spain.
2. Departamento de Geología, Museo Nacional de Ciencias Naturales-CSIC, 28006-Madrid, Spain.
3. Departamento de Geología, Facultad de Ciencias, Universidad de Salamanca, 37008-Salamanca, Spain.

* Javier.Lario@ccia.uned.es

Abstract

Effects of the 2010 Chilean earthquake and tsunami were evaluated at coastal sites between two zones of different coseismic deformation. Land deformation, run-up, inundation extent and deposit extent and thickness were measured in the field, providing insights into the processes and morphological changes associated with tsunami inundation and backwash. Three to five waves, of up to 10 m height, deposited several related layers along the coast, the thickness of these sandy deposits does not exceed 80 cm, and is generally less than 30 cm. Coseismic deformation measured by means of bio- and geomorphic markers agrees well both with model deformation and measured GPS. There is no relationship between the run-up height and the trend of coseismic deformation (uplift or subsidence), mainly because the effects of the tsunami were influenced locally by offshore bathymetry and coastal morphology.

Keywords: 2010 Chile tsunami, coseismic deformation, uplift, tsunami deposits, tsunami record

1. Introduction

On February 27th 2010 a Maule Region earthquake (at 06:34:14 UTC, with epicentre 35.909ºS, 72.733ºW, 35 km depth, USGS, 2016) with Mw 8.8 affecting central Chile, set off a tsunami that caused major damage to over 500 km of mainland coastline, as well as to several islands. Previously this area was identified as a seismic gap, with the potential to produce an earthquake of

Mw 8.0-8.5 (Ruegg et al., 2009). The earthquake and tsunami killed more than 577 inhabitants in the coastal regions of central Chile.

The earthquake was generated at the gently sloping fault that conveys the Nazca plate eastward and downward beneath the South American plate. The fault rupture, largely offshore, exceeded 100 km in width and extended nearly 500 km parallel to the coast. It began deep beneath the coast and spread westward, northward and southward. As it spread, the fault slip generated earthquake shaking and also deformed the ocean floor, setting off the tsunami along the fault-rupture area. Although the maximum water level observed in several places ranged from 10 to 12 m, and although 3 to 5 waves reached the coast during the next 4 hours, the sedimentary record and geomorphological changes recorded was less severe than other recent tsunami-generated by mega-earthquakes, like the 2004 Indian Ocean tsunami (Paris et al., 2007; Ontowirjo et al., 2013) or 2011 Tohoku-Oki tsunami (Mori et al., 2011; Goto et al., 2012a, b; Nakamura et al., 2012; Richmond et al., 2012; Tappin et al., 2012).

Different coseismic deformation (uplift or subsidence) was observed in different sectors of the coast and therefore an attempt was made to identify whether this land deformation controls the sedimentological pattern in each area. Coseismic coastal land-level changes have been estimated by intertidal organisms in different tectonic settings (subduction zones, strike-slip fault systems, and continental thrust belts) by mean of barnacles, corals, coralline algae, serpulids and molluscs (i.e. Plafker and Ward, 1992; Ortlieb et al., 1996; Ramirez-Herrera and Orozco, 2002; Ferranti et al. 2007; Shishikura et al. 2009; Castilla et al., 2010; Farías et al., 2010; Vargas et al., 2011; Melnick et al., 2012) but as has been pointed by Melnick et al. (2012): “few studies have focused on the distribution of such markers along an uplifted coastline, discussing the influence of local site effects on the accuracy of uplift measurements and the specific methodological aspects that may improve the reliability”.

After the 2010 Chile tsunami, several ITST groups (International Tsunami Survey Team, UNESCO) surveyed the effect of the tsunami, some focusing on the sedimentary record. In all cases tsunami run-up elevations and morphological changes were highly variable over short alongshore distances as a result local amplification effects due to alongshore variations in the tsunami wave heights, offshore bathymetry, shoreline orientations, and onshore topography (Fritz et al., 2011; Morton et al., 2011).

2. Methodology

From 17th to 30th March 2010 a survey of the tsunami sedimentary record was carried out in the context of the ITST (International Tsunami Survey Team, UNESCO). In order to study the tsunami impact, an area was selected where population was severely affected by the tsunami and where natural conditions were preserved. Two different coseismic deformation areas were selected from surface deformation models published by the California Institute of Technology just after the earthquake (Sladen, 2010). This model predicted uplift deformation in the Arauco Peninsula and stability in the Mataquito River area. With this premise, the two areas selected to survey were: a) Arauco Gulf and surrounding coast, inundated by the tsunami and also affected by coseismic uplift of up to 2.5 m, with emersion of the marine platform and tidal areas; and b) Mataquito River area, where coseismic subsidence was observed (Fig. 1). Later studies confirmed that because coseismic uplift tends to increase toward the trench, maximum amounts were modelled and observed in the southern rupture segment. The coastal subsidence was modelled and observed in the northern segment (Farías et al., 2010; Vigny et al., 2011).

Field survey methods were those applied in other post-tsunami surveys (Gelfenbaum and Jaffe, 2003; Goff et al., 2006; Jaffe et al., 2006). The terminology defined by the Tsunami Glossary published by the Intergovernmental Oceanographic Commission (2013) was used, as well as the Tsunami Survey Filed Guide published by same institution (Dominey-Howes et al., 2012). The terms that define the size of tsunami on the coast are: (a) run-up is the maximum ground elevation wetted by the tsunami on a sloping shoreline; (b) maximum inundation distance is the horizontal distance flooded by the wave (In the simplest case, the run-up value, a, is recorded at b); (c) flow depth is the depth of the tsunami flood over the local terrain height; and (d) tsunami height is the total elevation of the water free surface above a reference datum. Wave height and flow depth were measured using GPS, altimeter and tape, mainly using references such as marine remains and damage, e.g. to trees, houses, and fences, water level marks on walls and houses, and eye-witness testimony.

Run-up was measured by GPS following the maximum inundation line, identified from marine remains, garbage accumulated from the sea, accumulated vegetal remains and eye-witness testimony. The presence of marine fish and crabs in the hinterland were also recorded as markers of the inundation area. In some places a very thin layer of mud far above the last few vegetal and garbage remains marked the maximum inundation area limit. In some sites, displaced houses or boats in the hinterland were taken as markers of run-up. As with other researchers (Morton et al., 2011) the thickness of tsunami deposits was determined by digging short, shallow trenches along shore-normal and shore-parallel transects. Trenches were excavated to depths below pre-existing soil, the unaltered or eroded pre-tsunami surface. In some sites the lower limit was marked by artificial basement (concrete or asphalt).

Coseismic deformation was estimated using the Ortlieb et al. (1996) methodology, related to the presence of coralline algae. Coralline algae (lithothamnioids) located in the upper part of the infralittoral zone along rocky shorelines proved to be a useful indicator of rapid coastal uplift. As these encrusting algae cannot survive to desiccation they provide estimates of coseismic uplift. Once the algae die, their colour fades due to solar radiation (bleaching); a white band is observed, contrasting with the living algae immediately below. Measurement of the difference in elevation between this white fringe and the living algae provides a reliable indication of sudden uplift, as also observed in this area by Vargas et al. (2011). Coseismic deformation was also measured by altitude difference between tidal notches corresponding to the pre-seismic and post-seismic tidal levels. Subsidence was measured by reference to items such as harbours, telephone poles or fences and eyewitnesses testimonies, where the pre-seismic position was well known.

3. Results

3.1. Tsunami effects and land deformation in the Arauco Gulf area

The north and northwestern coast of Arauco Gulf and Peninsula, in the Bio-Bio Region of central Chile, some 100 km south of the earthquake epicentre (Fig. 1), were the most strongly affected by the tsunami following the earthquake. The greatest damage was to the fishermen villages of Llico and Tubul.

From west to east (Fig. 1b), the following features were recorded (summarized in Fig. 2 and Table 1): In Caleta Rubena (CR) there was no evidence of tsunami damage. Coseismic deformation was estimated by means of *Lithotamiun* algae to be around 1.80 to 2.00 m of uplift. There was also the presence of *Mytilus chilensis* (cholitos, small mussels) and other indicators of 0.80 cm of uplift above MHWL. In the entire area an uplifted marine platform can be observed. In Punta Lavapie (PL) there was no evidence of tsunami damage, but there was evidence of coseismic deformation of 1.80 to 2.00 m of uplift. In front of the village, the former wave-cut platform now lies about 2.00 above MHTL (Fig. 3). Malvenick et al. (2012) studied other mussel species (*Perumytilus purpuratus*) and estimate the uplift at this site between 1.67 to 1.91 m.

In the fishing village of Llico (Ll) the tsunami was very destructive. Maximum water level measured in Llico was +9.5 m MHWL, with a run-up of +7.5 m MHWL, with inland flooding in excess of 650 m. As a result of this flooding, a large number of houses were destroyed; some were swept up to 500 m inland (Fig. 4). In spite of the great energy of the event, the sedimentary record was only a centimetre-scale sandy layer, with the presence of crustaceans and some fish. There was no evidence of an erosional contact, even in areas where wooden houses were completely swept away. Eye-witnesses report the arrival of 3 waves, the last coming from Isla Santa Maria (north of Llico), plus one coming from the east (Tubul). Pre-tsunami aerial images show a 20 to 30 m wide sandy beach with no dunes present. Sediments transported by the tsunami consist of sand from the nearshore. The repeated sedimentary sequence, measured from bottom to top, consists of: 0.5 cm to 2.0 cm of massive fine sands and 4.0 to 7.0 cm laminated sands, that constitute a condensed sequence of the tsunami, recording three waves. Each wave generated a fine sand layer covered by a very fine, black millimetre-scale sand layer. The last sequence shows at its top a very fine millimetre-scale layer of mud and very fine sands. Usually there is no abrupt lower contact (erosional). Related to the coseismic deformation there is evidence of uplift (+1.60 to 1.80 m) measured from reference levels in the harbour.

In Tubul (Tu) village the tsunami was also very destructive, as was the tsunami generated by the 1960 earthquake. After the 1960 tsunami part of the village moved to *Tubul Nuevo (New Tubul),* but some years later houses were again built in *Tubul Viejo (Old Tubul)*, where most of the damage occurred from direct wave impact; New Tubul was affected by tidal channel flooding. More than 600 houses were destroyed. In this area 4 waves were observed, the last less energetic than the first ones. Maximum water level observed was +10.0 m MHWL, with a run-up of +4.5 m MHWL, and flooding that extended more than 900 m inland. Tubul village was flooded, as was the surrounding marshland. In Tubul and the Raqui River/tidal channel, the tsunami reached 3.9 km inland (Fig. 5). Coseismic uplift, marked by *Lithotamium algae*, uplifted shore platforms and tidal notches, and was estimated between +2.00 and +2.20 m. Due to uplift, the shoreline moved more than 100 m seawards. Although houses, boats, sea-wall boulders and vehicles were swept out some hundred meters, there is no evidence of erosion of surfaces and soils. Most of the sampling sites consist of 1-3 cm of fine sands with a very fine silty-sand as a cap. All surfaces in the area were covered by fish, shells and crustaceans. The most complete sedimentary record is located near the tidal channel, nearly 3 km inland, where the tsunami deposit (0.8 to 1.1 cm) consists of a constricted sequence, recording 4 layers corresponding to 4 waves (the first the largest, the following two smaller, with the last the smallest). Each layer consists of fine grey sand and very fine, black silty-sand (Fig. 6). In the entire area the presence of *pelillo* algae (*Gracilaria* sp.) marks the area flooded by the tsunami as well as the run-up. Although people report removing 40 to 50 cm of sand and mud from inside houses, there is no evidence of such deposits outside. Deposits generally consist of 2 to 8 cm of massive sands with the absence of an erosional base (Fig. 7).

The small settlement of Las Peñas (LP) was spared tsunami damage; the water level there never surpassed the village river-wall. There are remains of flooding near the Raqui River bridge where run-up was estimated at +2.5 m above MHWL. There is evidence of +1.80 m of uplift at this location.

From here to the town of Arauco (Ar) small coastal bays were flooded; as a result, some washover fans were deposited extending some 200 m inland, with the maximum inundation extent marked by plant debris, and with millimetre-scale sand deposits. In Arauco tsunami damage was slight, while earthquake damage was considerable, mainly because the village is some 8 to 20 m above MHWL and around 500 m from the coastline. While there was restricted damage to holiday housing near the beach, most of the coast is protected by dunes and forest and therefore most recreational homes were also protected.

Even though washover fans formed through interdune gaps, and flooding occurred near the village football playground (max. run-up +3.5 m), the sedimentary record was very scarce (3-4 cm. of massive sands). To the east in Laraquete (La) village, eye-witnesses reported three major waves and a smaller one, but there was scarce damage to some houses along the shoreline; some houses were flooded near the river/tidal channel. Maximum run-up was evaluated at 2.60 m MHWL. Field evidence indicated a coseismic uplift of +0.60 m.

3.2. Tsunami effects and land deformation in the Mataquito River area

Mataquito River is some 30-100 km north of the earthquake epicentre (Fig. 1). From south to north (Fig. 1b) the following features were recorded, summarized in Fig. 2:

At La Trinchera (LT-H), run up of +3.40 m in the Huenchullami River trough reached 3.2 km inland. At the Huenchullami River mouth, run-up was measured at + 8.5 m above MHWL. The sedimentary record ranges from 2 cm of fine sand (at +8.0 m) to 30 cm of sand and gravel near the shore. Return flow at La Trinchera crossing the coastal plain caused widespread erosion and scours of 1.5 m in depth. Large slabs of coastal road pavement were ripped off and transported seawards. Sections of concrete pipe were exposed and highway asphalt was eroded by the tsunami flow, suggesting very high velocities (Fig. 8a). Extensive inundation in this area suggests possible land subsidence (as was also observed by Morton, 2011).

The entire coast between Caleta Duao and Iloca was severely damaged by the tsunami. In Caleta Duao (CD) run-up reached +4.5 m above MHWL, and +3.10-3.40 m in a river channel outside the village, while flooding reached 3 km inland. In Iloca (Il) run-up was measured at +6.0 m above MHWL. Coseismic deformation, observed in the Mataquito River mouth as subsidence in flooded meadows and sunken electrical poles (Fig. 8b), was measured at -0.5 m. The spit barrier at the river mouth was breached; the entire area, previously pasture land, experienced flooding from the sea. The tsunami sedimentary record consists of 6 to 12 cm of sand, including centimetre-scale armoured mud. The entire sand body is covered by decimetre-scale armoured mud boulders, eroded from marsh deposits (Fig. 8c). All this area was inundated by the tsunami, with evidence of scour and erosion in multiple sites.

From Lipimávida (Li) to Pichibudi there is evidence of tsunami damage to properties but no evidence of coseismic deformation. Run-up was measured at +3.40 to 3.8 m above MHWL. The sedimentary record consists of 8 cm of massive, medium sands.

In Llico (Ll) some houses and restaurants were damaged by the tsunami. Here coseismic deformation in the form of 0.5 m of subsidence submerged the old bar that formerly closed Laguna La Torca, with progradation of a new bar inland (Fig. 8d). Run-up and maximum water level was measured at +2.7 m above MHWL; sediments accumulated after the tsunami consist of 0.85 m of massive black sand above concrete pavement.

In Bucalemu (Bu) damage was very sporadic; run-up was estimated at +2.70 m MHWL, subsidence at 0.5 m. A detailed study of tsunami flow at this site by Spiske and Bahlburg (2011) was based on the distribution of cobbles and boulders piled some days before the tsunami. In nearby Pichilemu (Pi), protected by coastal dunes, there was also scarce tsunami damage. Maximum run-up was measured at +4.60 m above MHWL. There was no evidence of coseismic deformation. Sediments consist of 4-6 cms of massive sands. The micropaleontology of sediments in this area was detailed by Horton et al. (2011).

4. Discussion

Coseismic deformation measured by means of geomorphological and biological markers in the Arauco Peninsula is similar to that measured with the same methodology by other authors (Castilla et al., 2010; Farías et al., 2010; Vargas et al., 2011; Melnick et al., 2012), but in the case of this study vertical coseismic deformation was associated with inundation extension and geomorpho-sedimentary features.

Fig. 9 shows the locations of measurements along the coast of vertical coseismic static deformation associated with the earthquake. Maximum uplift values were measured in the Arauco peninsula, with values as high as 2.00 to 2.20 m. Uplift decreasing towards the east of Arauco Gulf suggests a slight tilting of the coastal sector towards the non-deformed zone. A hinge line for coseismic uplift/subsidence change can be observed around 110-120 km from the trench, also observed by Farías et al. (2010), Vigny et al. (2011) and Moreno et al. (2012) using land-level changes inferred by GPS measures from the entire rupture zone studied.

Vigny et al. (2011) inferred static deformation and kinematics of the earthquake from GPS networks in central Chile. They found vertical displacements of up to 1.8 m of uplift at the Arauco peninsula tip, the land point closest to the trench. They also found subsidence southward and northward of Constitución. Their estimated values in the area are within the range established in this study from geomorphological, biological and anthropogenic markers - an indication that this methodology provides an effective measure of vertical coseismic deformation after an earthquake in areas without a GPS network, and also confirms preliminary GPS data obtained in areas covered by this technology.

The largest values of tsunami wave height were measured in Arauco peninsula, estimated at 9.5 m. Values of maximum tsunami height lack a clear pattern, probably as a result of alongshore variations in tsunami wave heights associated to possible amplification effects related to offshore bathymetry, shoreline orientation and onshore topography.

Stable and subsiding areas of Mataquito River sector displayed more erosion features and displacement of boulders, even with smaller values of tsunami run-up than in the Arauco Peninsula. Only in areas protected by dunes or forest was the effect of the tsunami negligible.

As a result of uplift, some marine platforms were exposed and the coastline retreated some hundreds of meters, although this coseismic deformation in some places of the Gulf of Arauco (Llico and Tubul) was largely inundated. Morton et al. (2011) studied the area affected by the tsunami from Talcahuano to La Trinchera and concluded that embayment did not necessarily amplify water levels of the 2010 tsunami. In the case of this study, embayment areas of Lico and Tubul in Gulf of Arauco present both the largest inundation area and highest water level observed, although all the area was uplifted. Wave height in this coastal sector was amplified by the shape of the coast and its location south of the epicentre, facing the direction of wave propagation (parallel to the wave front). Moreover, if this coastal sector had not been uplifted, or had subsided, the tsunami effect would have been more severe and destructive. Fritz et al. (2011) also concluded that the coastal uplift during the earthquake prior to tsunami arrival reduced the tsunami impact.

In most areas deposits ranging in size from mud to sand reached a maximum thickness of 20 cm and generally thinner inland. Sandy tsunami deposits are characterized by massive or parallel laminated sand and silt. In coastal marsh areas, tsunami sand includes ripped-up mud clasts. Tsunami deposits generally range from one to a few units, with multiple layers observed mainly close to the shoreline. This agrees with the number of waves, 3 to 5, which arrived at the study sites. Thicker sand deposits (up to 80 cm) were found in subsiding areas and close to spit bars or dunes that supplied sediment. This was also observed in the 2011 Tohoku-Oki tsunami, where the average thickness of sand deposits was 30 cm (Goto et al., 2012c). Also, in the more destructive 2004 Indonesia tsunami, sand deposits of up to 82 cm thickness were found in low topography areas, but most sand deposits were thinner than 30 cm (Paris et al., 2007). In the Arauco Peninsula most sediments were back-washed into the sea; uplift of the area increased this backwash through potential energy amplification triggered by the differential altitude of the pre- and post-tsunami shoreline after coseismic deformation.

5. Conclusions

The 2010 Chile earthquake generated coseismic land deformation (uplift and subsidence) that in coastal areas was evaluated by means of bio- and geomorphic markers. This method of evaluating the geological effects was found to be a valid methodology for quantifying ground deformation in areas lacking a fixed GPS network or pre-earthquake GPS data. In addition, the survey of geological effects of the tsunami generated by the earthquake showed that run-up, maximum inundation and sediment thickness and size were not as large as in other destructive tsunamis generated by similar earthquakes, such as the 2004 Indonesia tsunami or 2011 Tohoku-Oki tsunami. It is probable that the severity was reduced by both earthquake-caused coseismic uplift of up to 2.00 m along some parts of the coastline, and by the low tide level at the time of the tsunami.

As noted by Goto et al. (2012c), the explanation of the average thickness of the tsunami deposits (in the case of this study less than 20 cm) remains a challenge. In the uplifted Arauco sector, the coseismic deformation seems to have increased backwash of remobilized sediments, leaving the observed thin deposits. Whereas in the stable and subsiding sites of the Mataquito River, sand deposits, pebble and cobble sediments are thicker.

Acknowledgements

Financial support by Spanish Projects CGL2013-42847-R and CGL2012-33430. It is a contribution to UNESCO-International Geoscience Program Project 639, INQUA Coastal and Marine Processes Commission and INQUA Focus Area on Paleoseismicity and Active Tectonics.

References

Castilla, J.C., Manríquez, P., Camaño, A. (2010). Effects of rocky shore coseismic uplift and the 2010 Chilean mega-earthquake on intertidal biomarker species. Marine Ecology Progress Series 418, 17-23.

Dominey-Howes, D., Dengler, L., Dunbar, P., Kong, L., Fritz, H., Imamura, F., McAdoo, B., Satake, K., Yalciner, A., Yamamoto, M., Yulianto, E., Koshimura, S., Borrero, J. (2012). International Tsunami Survey Team (ITST) Post-Tsunami Survey Field Guide. 2nd Edition. UNESCO-IOC, Paris.

Farías, M., Vargas, G., Tassara, A., Carretier, S., Baize, S., Melnick, D., Bataille, K. (2010). Land-level changes produced by the Mw 8.8 2010 Chilean earthquake. *Science* 329, 916.

Ferranti, L., Monaco, C., Antonioli, F., Maschio, L., Kershaw, S., Verrubbi, V. (2007). The contribution of regional uplift and coseismic slip to the vertical crustal motion in the Messina Straits, southern Italy: Evidence from raised late Holocene shorelines. *J. Geophys. Res*. 112, B06401, 1-23.

Fritz, H.M., Petroff, C.M., Catalan, P.A., Cienfuegos, R., Winckler, P., Kalligeris, N., Weiss, R., Barrientos, S.E., Meneses, G., Valderas-Bermejo, C., Ebeling, C., Papadopoulos, A., Contreras, M., Almar, R., Dominguez, J.C., Synolakis, C. (2011). Field survey of the 27 February 2010 Chile tsunami. *Pure and Applied Geophysics* 168, 1989-2010.

Gelfenbaum, G., Jaffe, B. (2003). Erosion and sedimentation from the 17 July 1998 Papua New Guinea tsunami. *Pure and Applied Geophysics* 60, 1969–1999.

Goff, J., Liu, P., Higman, B., Morton, R., Jaffe, B., Fernando,H., Lynett, P., Fritz,H., Synolakis, C. (2006). The December 26, 2004 Indian Ocean tsunami in Sri Lanka. *Earthquake Spectra* 22, S155–S172.

Goto, K., Chagué-Goff, C., Goff, J., Jaffe, B. (2012c). The future of tsunami research following the 2011 Tohoku-oki event. *Sedimentary Geology* 282, 1-13.

Goto, K., Fujima, K., Sugawara, D., Fujino, S., Imai, K., Tsudaka, R., Abe, T., Haraguchi, T. (2012b). Field measurements and numerical modeling for the run-up heights and inundation distances of the 2011 Tohoku-oki tsunami at Sendai Plain, Japan. Earth, Planets and Space, 64, 1247-1257.

Goto, K., Sugawara, D., Ikema, S., Miyagi, T. (2012a). Sedimentary processes associated with sand and boulder deposits formed by the 2011 Tohoku-oki tsunami at Sabusawa Island, Japan. Sedimentary Geology, 282, 188-198.

Horton, B.P., Sawai, Y., Hawkes, A.D., Witter, R.C. (2011). Sedimentology and paleontology of a tsunami deposit accompanying the great Chilean earthquake of February 2010. *Marine Micropalentology* 79, 132-138.

Intergovernmental Oceanographic Commission (2013). Tsunami Glossary. Paris, UNESCO. IOC Technical Series, 85.

Jaffe, B.E., Borrero, J.C., Prasetya, G.S., Peters, R., McAdoo, B., Gelfenbaum, G., Morton, R., Ruggiero, P., Higman, B., Dengler, L., Hidayat, R., Kingsley, E., Kongko, W., Lukiyanto ; Moore, A., Titov, V., Yulianto, E. (2006). The December 26, 2004 Indian Ocean tsunami in northwest Sumatra and offshore islands. *Earthquake Spectra* 22, S3, 105–S136.

Melnick, D., Cisternas, M., Moreno, M., and Norambuena, R. (2012). Estimating coseismic coastal uplift with an intertidal mussel: calibration for the 2010 Maule Chile earthquake (Mw=8.8). *Quaternary Science Reviews* 42, 29-42.

Moreno, M.; Melnick, D.; Rosenau, M.; Baez, J.C.; Klotz, J.; Oncken, O.; Tassara, A.; Bataille, K.; Chen, J.; Socquet, A.; Bevis, M.; Bolte, J.; Vigny, C.; Brooks, B.; Simons, M.; Grund, V.; Smalley, R.; Carrizo, D.; Bartsch, M.; Hase, H. (2012). Toward understanding tectonic control on the Mw 8.8 2010 Maule Chile earthquake. *Earth and Planetary Science Letters* 321, 152-165.

Mori, N., Takahashi, T., Yasuda, T., Yanagisawa, H. (2011). Survey of 2011 Tohoku earthquake tsunami inundation and run-up. Geophysical Research Letters, 38, L00G14.

Morton, R.A., Gelfenbaum, G., Buckley, M.L., Richmond, B.M. (2011). Geological effects and implications of the 2010 tsunami along the central coast of Chile. *Sedimentary Geology* 242, 34-51.

Nakamura, Y., Nishimura, Y., Putra, P.S. (2012). Local variation of inundation, sedimentary characteristics, and mineral assemblages of the 2011 Tohoku-oki tsunami on the Misawa coast, Aomori, Japan. Sedimentary Geology, 282, 216-227.

Ontowirjo, B., Paris, R., Mano, A. (2013). Modeling of coastal erosion and sediment deposition during the 2004 Indian Ocean tsunami in Lhok Nga, Sumatra, Indonesia. Natural Hazards, 65, 1967-1979.

Ortlieb, L.; Barrientos, S.; Guzman, N. (1996). Coseismic coastal uplift and coralline algae record in northern Chile: the 1995 Antofagasta earthquake case. *Quaternary Science Reviews* 15, 949-960.

Paris, R., Lavigne, F., Wassmer, P., Sartohadi, J. (2007) Coastal sedimentation associated with the December 26, 2004 in Lhok Nga, west Banda Aceh (Sumatra, Indonesia). *Marine Geology* 238, 93-106.

Plafker, G.; Ward, S.N. (1992). Backarc thrust faulting and tectonic uplift along the Caribbean Sea Coast during the April 22, 1991 Costa Rica earthquake. *Tectonics* 11, 709-718.

Ramírez-Herrera, M.T.; Orozco, J.J.Z. (2002). Coastal uplift mortality of coralline algae caused by a 6.3 Mw earthquake, Oaxaca, Mexico. *Journal of Coastal Research* 18, 75-81.

Richmond, B., Szczuciński, W., Goto, K., Sugawara, D., Witter, R.C., Tappin, D.R., Jaffe, B., Fujino, S., Nishimura, Y., Chagué-Goff, C., Goff, J. (2012). Erosion, deposition, and landscape change on the Sendai coastal plain, Japan resulting from the March 11, 2011 Tōhoku-oki tsunami. *Sedimentary Geology* 282, 27-39.

Ruegg, J.C., Rudloff, A., Vigny, C., Madariaga, R., De Chabaliera, J.B., Campos, J., Kausel, E., Barrientos, S., Dimitrov, D. (2009).Interseismic strain accumulation measured by GPS in the seismic gap between Constitución and Concepción in Chile. *Phys. of the Earth and Planetary Interiors* 175, 78-85.

Shishikura, M., Echigo, T., Namegaya, Y. (2009), Evidence for coseismic and aseismic uplift in the last 1000 years in the focal area of a shallow thrust earthquake on the Noto Peninsula, west-central Japan. *Geophys. Res. Lett*. 36, L02307, 1-5.

Sladen, A. (2010). Preliminary Result 02/27/2010 (Mw 8.8), Chile. http://www.tectonics.caltech.edu/slip_history/2010_chile/. Last view February 09, 2016.

Spiske, M.; Bahlburg, H. (2011). A quasi-experimental setting of boulder transport by the 2010 Chile tsunami (Bucalemu, Central Chile). *Marine Geology* 289, 72-85.

Tappin, D.R., Evans, H.M., Jordan, C.J., Richmond, B., Sugawara, D., Goto, K. (2012). Coastal changes in the Sendai area from the impact of the 2011 Tōhoku-oki tsunami: interpretations of time series satellite images and helicopter-borne video footage. *Sedimentary Geology* 282, 151-174.

USGS (2016). Earthquakes Hazards Programe. M8.8 - offshore Bio-Bio, Chile. http://earthquake.usgs.gov/earthquakes/eventpage/usp000h7rf#general_executive, February 09, 2016.

Vargas, G., Farias, M., Carretier, S., Tassara, A., Baize, S., Melnick, D. (2011). Coastal uplift and tsunami effects associated to the 2010 Mw8.8 Maule earthquake in Central Chile. *Andean Geology* 38, 219-238.

Vigny, C., Socquet, A., Peyrat, S., Ruegg, J.C., Métois, M., Madariaga, R., Morvan, S., Lancieri, M., Lacassin, R., Campos, J., Carrizo, D., Bejar-Pizarro, M., Barrientos, S., Armijo, R., Aranda, C., Valderas, M.C., Ortega, I., Bondoux, F., Baize, S., Lyon-Caen, H., Pavez, A., Vilotte, J.P., Bevis, M., Brooks, B., Smalley, R., Parra, H., Baez, J.C., Blanco,M., Cimbaro, S., Kendrick, E. (2011).The 2010 Mw8.8 Maule megathrust earthquake of Central Chile monitored by GPS. *Science* 331, 1417-1421.

Site	Latitude	Longitude	Runup	Inundation	Coseismic deformation	Sedimentation	Marker
Caleta Rubena	37°10'25.93"S	73°36'49.81"W			1.80-2.00 m		BM
Punta Lavapie	37° 9'0.15"S	73°34'35.33"W			1.80-2.00 m		BM, GM, H
Llico	37°11'28.81"S	73°34'5.10"W	5.50 m			4 cm sand	DL
Llico	37°11'37.09"S	73°33'52.91"W	7.50 m (t.h.)				S, TM
Llico	37°11'52.69"S	73°34'7.45"W	5.00 m	663 m			DL, EW
Llico	37°11'38.38"S	73°33'45.58"W				1.60-1.80 m	H
Llico	37°11'37.29"S	73°33'53.82"W	12 m (t.h.)			5 cm sand	S
Llico	37°11'33.82"S	73°34'12.59"W	11 m				DL
Tubul (cementery)	37°12'30.26"S	73°30'59.46"W	4.50 m	87 m		5 cm sand	DL, WF
Tubul	37°14'10.78"S	73°28'52.97"W		3.2 km (tidal channel)		3 cm sand and mud	A, DL, C, F
Tubul	37°13'39.19"S	73°26'58.02"W		940-1120 m			DL, F, C
Tubul	37°13'34.84"S	73°26'8.74"W			2.00 m		BM, GM
Las Peñas	37°15'45.10"S	73°26'21.53"W	4.00 m	2.5 km			DL, F, A, C
Las Peñas	37°15'27.18"S	73°26'11.73"W	2.50 m		1.80 m		DL, A, EW, H
Las Peñas-Arauco	37°14'38.49"S	73°25'10.18"W	5.00 m	328 m		Washover fan	DL
Arauco	37°14'29.11"S	73°19'17.58"W	3.50 m	480 m		4 cm sand	A, EW
Laraquete	37° 9'55.26"S	73°11'16.89"W	2.60 m		0.60 m		A, EW
La Trinchera	35° 7'6.31"S	72°12'17.00"W	1.80-2.00 m		-0.50 m	25 cm sand, armoured mud	DL, WL, DT
Huenchelami	35° 7'19.87"S	72°12'18.70"W	8.5 m			2 cm sand	DL
Caleta Duao camping	34°52'51.86"S	72° 9'17.67"W	3.30 m			12 cm sand	DL
Caleta Duao	34°53'21.54"S	72° 8'52.82"W	4.50 m	2.7 km (in stream)		4 cm sand	DL, A
Iloca	34°56'32.50"S	72°11'10.05"W	6.00 m				
Mataquito River mouth	34°59'3.18"S	72°10'50.09"W			-0.50	20 cm sand, armoured mud,	PP, DL
Lipimavida-	34°51'27.87"S	72° 8'44.34"O	3.80 m		Stable	8 cm sand	DL
Llico	34°45'15.16"S	72° 5'4.80"O			-0.50 m		
Bocalemu	34°38'27.00"S	72° 2'37.95"W	2.70		-0.50 m		EW
Pichilemu	34°23'5.73"S	72° 0'16.57"W	4.60 m		Stable	2.00-5.00 cm sand	DL, EW

Table I. Studied sites. Markers: BM: Biomarker; GB: Geomarker, H: Harbor reference; DL: Debris line; S: Seed in trees; TM: Tree mark; EW: Eyewitness; WF: washover fan; C: Crab; F: Fish; A: Algae; DT: Drainage tubes; PP: Phone poles.

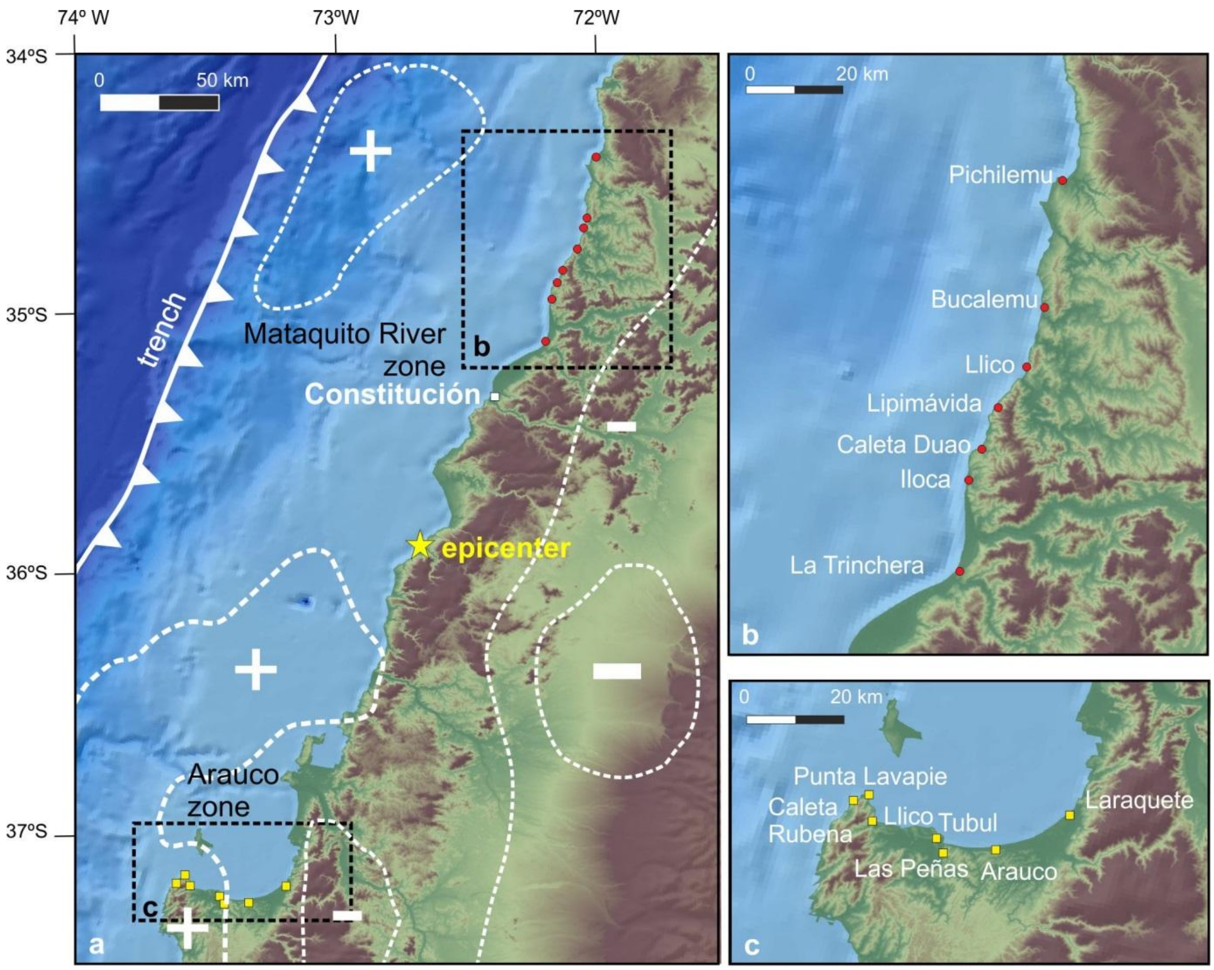

Figure 1. Location map of the two areas studied. Land deformation (uplift, +; subsidence, -) from surface deformation models published just after the earthquake by Sladen (2010).

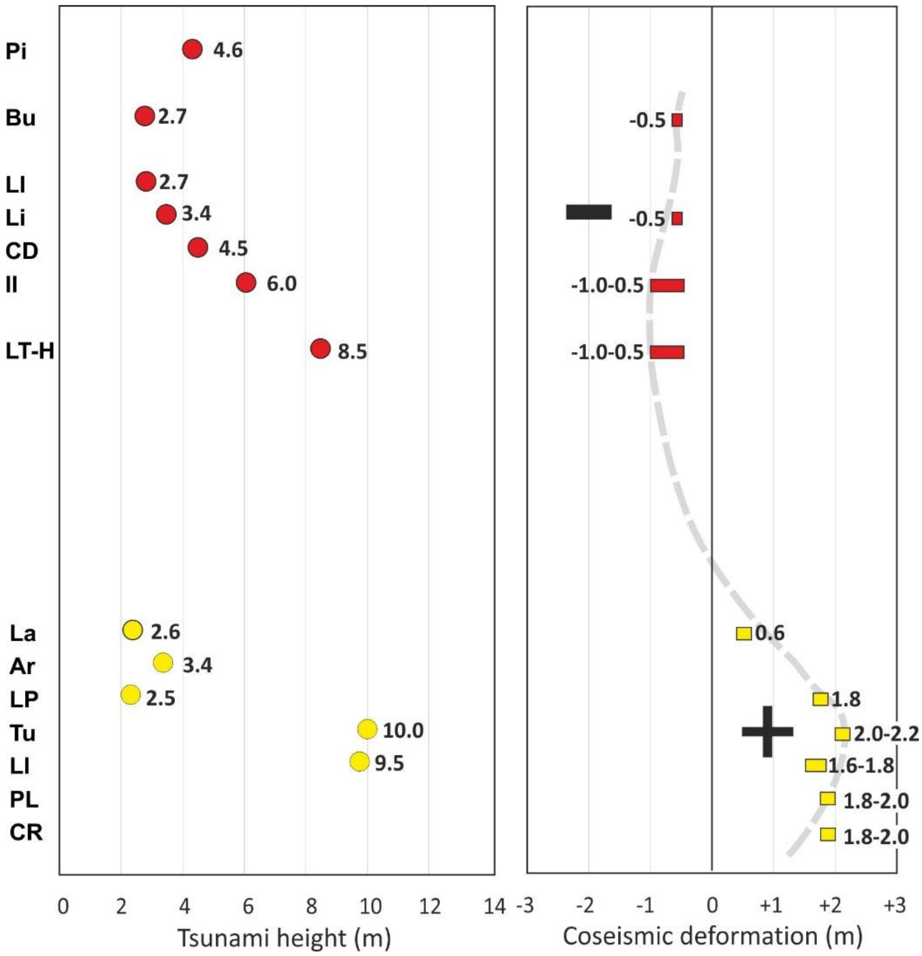

Figure 2. Run-up height and coseismic deformation at the studied sites (see Fig. 1). See sites abbreviations in text.

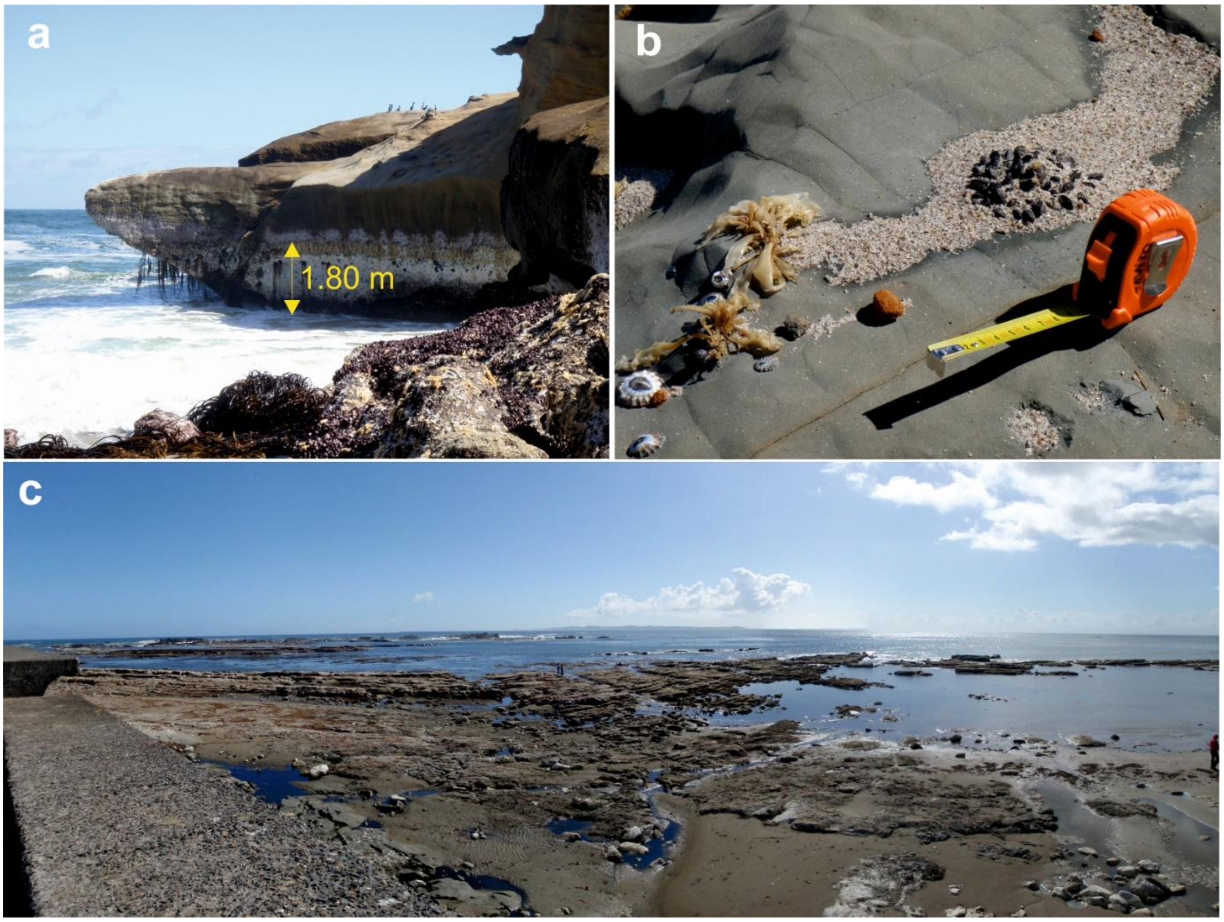

Figure 3. **a**. Caleta Rubena, evidence of coseismic deformation, 1.80 to 2.00 m of uplift by mean of *Lithothamnium* alga. **b.** Presence of *Mytilus chilensis* (cholitos) at 1.20 cm up MHWL. **c.** Punta Lavapie**:** evidence of coseismic uplift: the former shore platform currently emerges about 2.00 above MHWL.

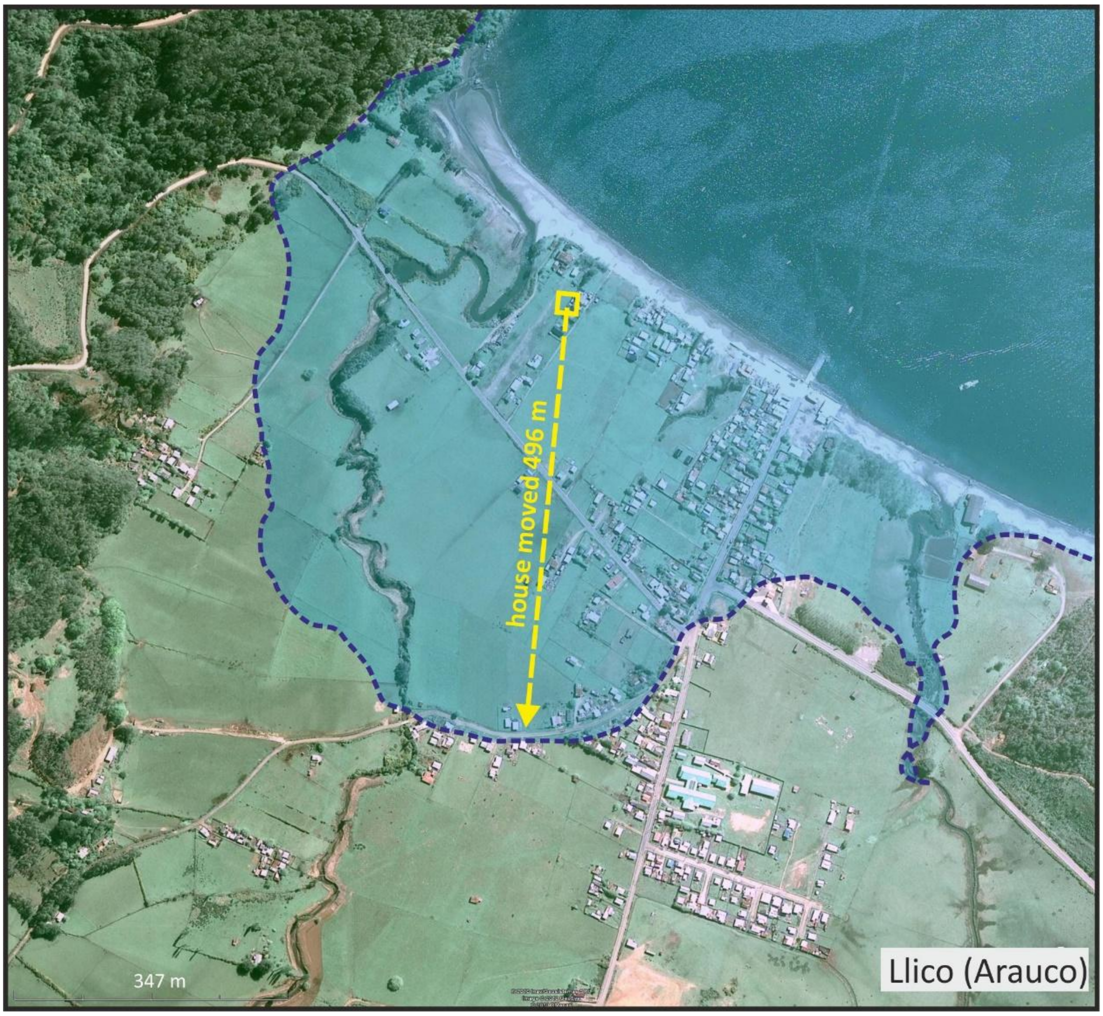

Figure 4. Area in Llico (Arauco Peninsula) devastated and inundated by the tsunami, where wooden houses were moved up to 500 m from original sites.

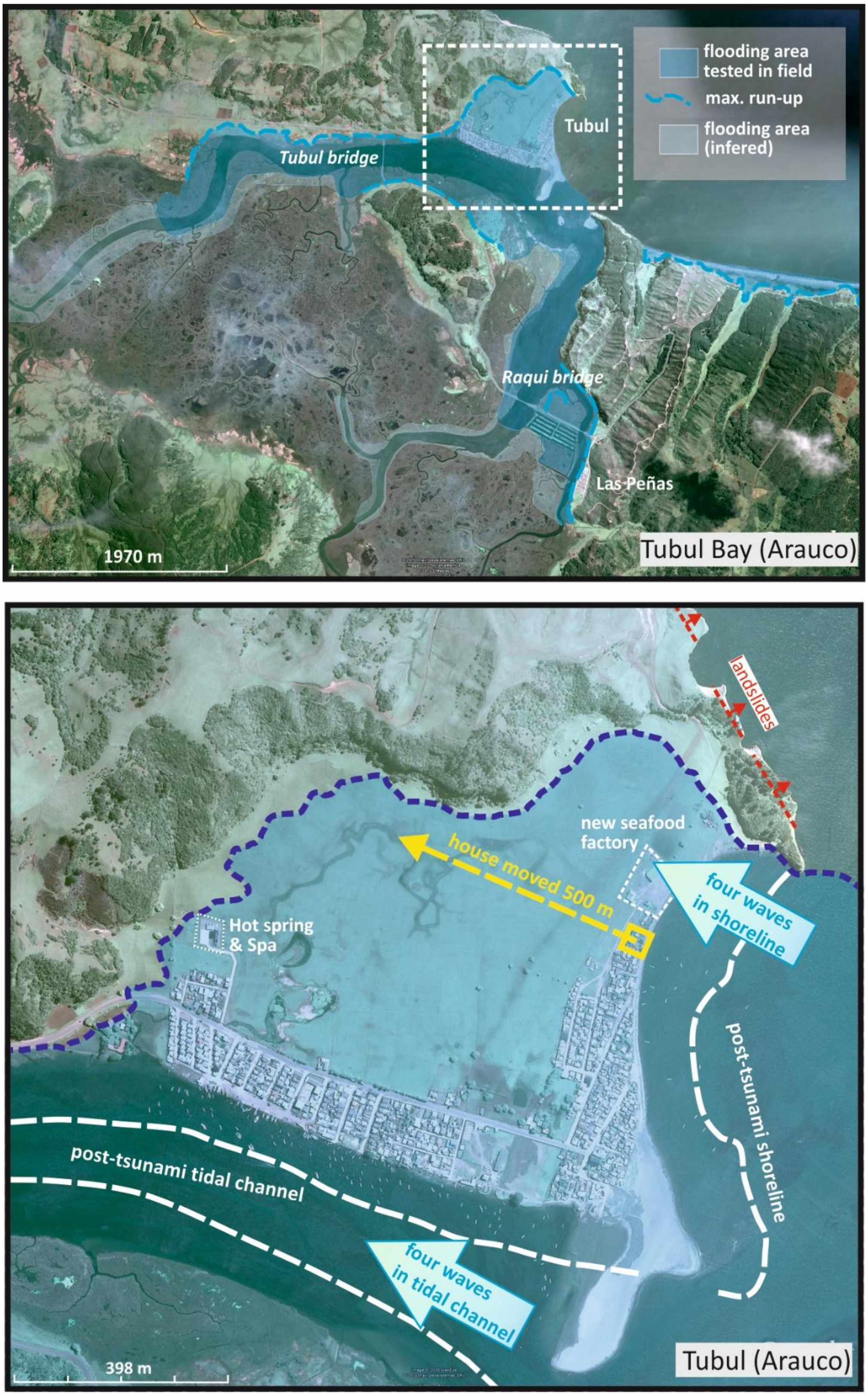

Figure 5. Area in Tubul (Arauco Peninsula) flooded by the tsunami where wooden houses were moved up to 900 m from original sites.

Figure 6. Tsunami deposits at +3.0 m above MHWL, past Tubul Bridge, associated with the tidal channel. a. 0.6 m of water depth, marked by presence of pelillo (Gracilaria sp.). b. Tsunami deposit (0.8 to 1.1 cm) showing a constricted sequence recording 4 layers corresponding to 4 waves (the first the largest, followed by two smaller, and last the smallest). Each layer consists of fine grey sand and very fine black silty-sand. **c.** Differential mud-cracking in the diverse layers. **d.** Detail of tsunami layers.

Figure 7. **a.** Tsunami deposit near seafood factory in Tubul. Note absence of erosion. **b.** Tsunami deposit (detail): 4-5 cm of fine massive sands lacking internal structure. Net contact. **c.** Tsunami deposit at surface. Note presence of *Nephrops norvegicus* and small fish in the deposit (1.1 km from shoreline).

Figure 8. **a.** Sections of concrete pipe exposed and highway asphalt eroded by tsunami flow, suggesting very high velocities, La Trinchera; **b.** 0.5 m of subsidence estimated at Mataquito River mouth, measured by means of inundated meadows and sunken electrical poles (note the isolated pole in middle of picture); **c.** At the Mataquito River mouth the entire sand body is covered by decimetre-thick armoured mud boulders, all eroded from meadow deposits; **d.** In Llico there is evidence of coseismic deformation, 0.5 m of subsidence, submerging the bar that previously closed Laguna La Torca.

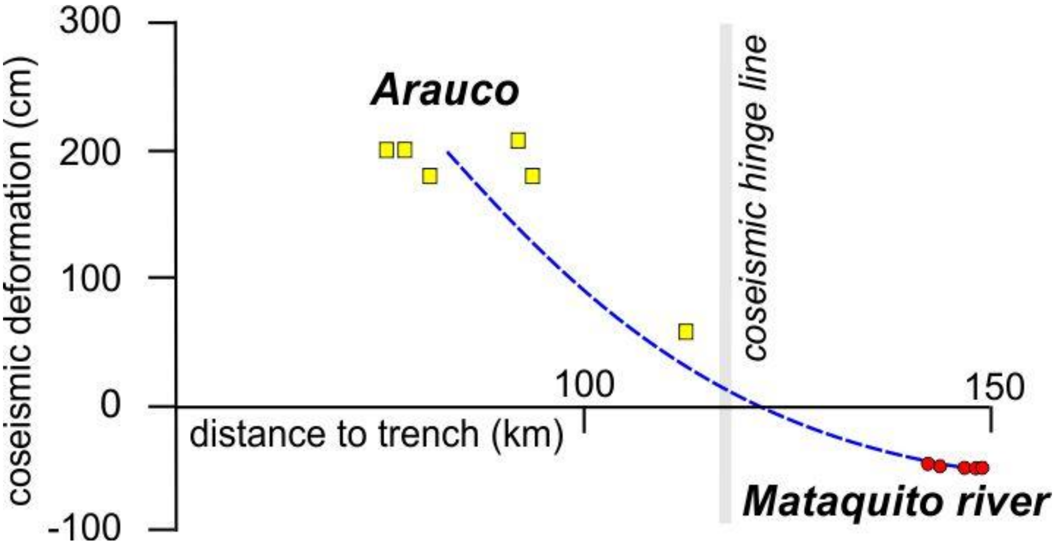

Figure 9. Location along the coast of measurement of vertical coseismic movement associated with the rupture area.